


RESEARCH ARTICLE

# Kinematic analysis of overconstrained manipulators with partial subspaces using decomposition method

Özgün Selvi 

Mechanical Engineering Department, Çankaya University, Ankara, Turkey  
E-mail: [ozgunselvi@cankaya.edu.tr](mailto:ozgunselvi@cankaya.edu.tr)

**Received:** 8 April 2021; **Revised:** 11 August 2021; **Accepted:** 23 August 2021; **First published online:** 30 September 2021

**Keywords:** overconstrained, decomposition method, parallel manipulator

## SUMMARY

Overconstrained manipulators in lower subspaces with unique motions can be created and analyzed. However, far too little attention has been paid to creating a generic method for overconstrained manipulators kinematic analysis. This study aimed to evaluate a generic methodology for kinematic analysis of overconstrained parallel manipulators with partial subspaces (OPM-PS) using decomposition to parallel manipulators (PMs) in lower subspaces. The theoretical dimensions of the method are depicted, and the use of partial subspace for overconstrained manipulators is portrayed. The methodology for the decomposition method is described and exemplified by designing and evaluating the method to two overconstrained manipulators with 5 degrees of freedom (DoF) and 3 DoF. The inverse kinematic analysis is detailed with position analysis and Jacobian along with the inverse velocity analysis. The workspace analysis for the manipulators using the methodology is elaborated with numerical results. The results of the study show that OPM-PS can be decomposed into PMs with lower subspace numbers. As imaginary joints are being utilized in the proposed methodology, it will create additional data to consider in the design process of the manipulators. Thus, it becomes more beneficial in design scenarios that include workspace as an objective.

## 1. Introduction

In recent years, there has been an increasing interest in parallel manipulators (PMs). Numerous PMs have been proposed, and kinematics and dynamics methods are suggested and applied [1]–[5]. There has been a particular interest in lower mobility parallel manipulators (LMPMs) due to their advantages as having simpler mechanical designs, larger workspace, error tolerance, agility and robustness. Overconstrained parallel manipulators (OPMs) are subclass for LMPMs. The overconstrained manipulators are arranged due to their subspaces. Moreover, the overconstrained manipulators are perfect candidates for the job done by LMPMs because the desired motion of the end effector is in a subspace.

Research has been done for the overconstrained manipulators in the areas such as structural synthesis, type synthesis, kinematic analysis, dynamic analysis, stiffness, force analysis and dynamic analysis. In the structural synthesis, the needed number of joints and their configurations are found. Intuition, screw theory, or group theory are the most common methods. Gogu [6] Suggested a methodology for the structural synthesis of fully isotropic OPMs. In their research, Kong and Gosselin [7] proposed a screw theory-based virtual chain approach for the type synthesis of PMs where some are overconstrained. Dai *et al.* [8] prompted a screw theory based mobility formulation for overconstrained parallel mechanisms. Lee and Herve [9] created a lie group approach for the structural synthesis of 4 DoF (3T1R) OPMs with uncoupled actuation. Hu [10] investigated the Exechon PM, expressed kinematically identical overconstrained and non-overconstrained manipulators and compared them with the Exechon PM. Structural synthesis of overconstrained manipulators with partial subspaces is described with a methodology based on unit screws is described in the work of Selvi [11].

Some overconstrained manipulators are suggested by researchers [12]–[15], and kinematic analysis is done by analytical and geometric methods. Yan *et al.* [12] suggested two overconstrained 2-RPU&SPR PMs and compared their kinematic behaviors, workspace and dexterity. They also made a comparative stiffness analysis for the same two manipulators [16]. Yan *et al.* [13] proposed a 3 DoF overconstrained manipulator. Using an analytical method, it analyses the manipulator's kinematics, recommends an algorithm for the manipulator's workspace analysis, then finds the reachable workspace. Li *et al.* [14] proposed a 2R1T OPM, namely Hex4. After the kinematic analysis is done, the link parameters are optimized for a better transmission workspace. Arian *et al.* [15] provides a Schönflies motion generator with infinite tool rotation in their research. The system is overconstrained, and the kinematic problem is investigated for the position, velocity and acceleration of the mechanisms. Singularity analysis and dynamic models are also developed for the system. Kinematic analysis of a 5 DoF overconstrained manipulator for rehabilitation is described in the work of Selvi and AL-Dulaimi [17].

Also, dynamic analysis of OPMs is done by several researchers. Sharifzadeh *et al.* [18] claim to have obtained a closely realistic dynamic model of 3 DoF translational OPM Tripteron using the white box and black box model and genetic algorithm. For the overconstrained 2PUR–PSR PM, researchers [19] described two dynamic models with and without constrained forces/moments using the Newton–Euler approach and natural orthogonal complement method. Arian *et al.* [15] carried out the kinematic and dynamic analysis of overconstrained manipulator Tripteron through Newton–Euler approach. Research also has been done related to the force and stiffness relations of the overconstrained manipulators. Xu *et al.* [20] carried out a screw theory based method considering the link elastic deformations and stiffness matrix for analyzing the force relation of overconstrained LMPMs. Liu *et al.* [21] reviewed the methods for the force analysis of OPMs. They discussed the problem of passive and active OPMs' statically indeterminacy. They also prompted a universal method for those two kinds based on the screw theory. Dynamic analysis of a 5 DoF overconstrained manipulator is done with the decomposition of the partial subspaces is described in the work of Selvi and Yilmaz [22].

Based on linear algebra and screw theory, Liu *et al.* [23] presented a systematic approach for force/motion transmissibility of redundantly actuated and OPMs. Comparing both types, they found out that the effect of being overconstrained has little concerning having actuation redundancy. To overcome the statically indeterminate problem in the force analysis of OPM's, Xu *et al.* [24] investigates the presence of the linearly dependent overconstrained wrenches. They reformulate the deformation compatibility equations between the overconstrained wrenches and describe the principle force model for OPMs and analyze these on a 2RPU–SPR OPM.

Hu and Huang [25] provided a kinetostatic model for an overconstrained LMPM with 2-RPU+UPR joint leg configuration. Using this kinetostatic model, the stiffness and the deformations of links are exemplified. Yang *et al.* [26] proposed a modeling method for the elastostatic stiffness of OPMs using screw theory and applying the method to 2UPR–RPU PMs. Zhang and Fang [27] proposed a 1T2R OPM with 2RPU–2SPR joint configuration and they calculated the linear and angular stiffness of the PM to find distributions law of the performance indices of redundantly actuated and overconstrained. Li *et al.* [28] proposed a method for the analytical elastostatic stiffness modeling of OPMs. They elaborated geometric algebra along with strain energy. They also showed proof of concept comparison with finite element methods. In the study of Zhao *et al.* [29], the reachable workspace of an OPM with 2RPU&SPR joint configuration is investigated by using an analytical approach. Decomposition is used to divide a closed chain system into serial chains for the direct task and path planning of manipulators in the work of Han and Amato [30]. A random loop generator is presented and used for the kinematic analysis of closed-loop chains by Cortes *et al.* [31]. The selection of active and passive links is essential and is mainly used for path planning for probabilistic road mapping.

Overconstrained manipulators for lower subspaces can be created and analyzed for different tasks with unique motions. However, far too little attention has been paid to creating a generic method for OPM's kinematic analysis. This study aimed to evaluate a generic methodology for kinematic analysis of overconstrained parallel manipulators with partial subspaces (OPM-PS) and validate the method with examples. The essay has been organized in the following way. It begins by laying out the theoretical

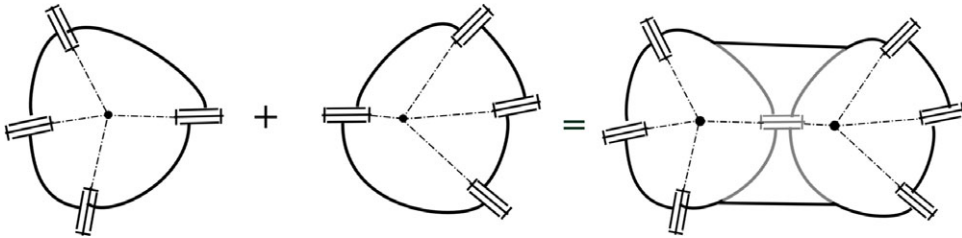


**Figure 1.** Bennett double spherical overconstrained mechanism.

dimensions of the research and looks at how the partial subspaces can be used to describe an overconstrained manipulator. The new method that decomposes the mechanism into multiple lower subspace manipulator loops is presented. The methodology is then exemplified by designing and evaluating an overconstrained manipulator with a 5 DoF overconstrained manipulator. The inverse kinematic analysis for position analysis is shown. The Jacobian is derived for the system, and the inverse velocity task is described. The workspace calculation for the methodology is also described, and some numerical examples are depicted. Additionally, the procedure is applied for a 3 DoF (2T1R) PM. Finally, the methodology and examples are discussed.

## 2. Decomposition Method in OPMs

Mechanisms that belong to a subspace are described to be overconstrained. Depending on the geometry of links, these subspaces can have partial subspaces, which can be helpful in the kinematic analysis of overconstrained manipulators of this type.

Bennett [32] proposed a method for creating an overconstrained mechanism by combining two mechanisms by using an intersecting joint. Removing the joint is possible due to the overconstrained subspace property (Fig. 1). These mechanisms behave in how the motion has both independent parts at each subspace and intersecting motion. The resulting 6R mechanism can be defined with two partial spherical subspaces with an imaginary joint, as shown in Fig. 1.

In Selvi's (2012) work, this method was generalized and used for the structural design of PMs. Several manipulators are generated using the method. Kinematic analysis and synthesis of the resulting mechanisms are done by reversing the idea and decompose the mechanism with an imaginary joint. The output of the first mechanism with a lower subspace will be input for the second one with another lower subspace. The partial subspaces for overconstrained manipulators are listed as spherical, planar, cylindrical, line and plane with just translation. An overconstrained manipulator generated using the combination method (Selvi 2012) will include subspaces with lower subspace degrees. In that case, the decomposition method can be used to separate the manipulator into two subspaces by adding imaginary joints. Imaginary joints are selected according to the intersection motion of the partial subspaces. The overconstrained manipulator is simulated as two manipulators where one's input is the other manipulator's output. One of the manipulators will include passive joints, and the other will include active joints. Also, end effector motion will belong to these two subspaces and their intersection motion.

The manipulator to be analyzed is an  $N$  DoF manipulator (Fig. 2(a)) and should be dividable into two partial subspaces (Fig. 2(b)).  $J$  imaginary joints are added to the manipulator (Fig. 2(c)).  $J$  is determined by investigating each leg of the manipulator, in each leg, the added joint should not create any redundancy on the newly created manipulator in the upper subspace. The type and direction of the imaginary joints should be selected according to the intersection motion of the subspaces. The first section below will be defined with an  $N$  DoF manipulator that consists of the real base and a virtual platform (Fig. 2(e)).  $N$  DoF controls the motion of the moving platform and controls accompanying links to the platform that transmits motion to the second section (upper part) of the manipulator. The motion of these links will be the input for the second section. The second section is described with a manipulator with  $J$  DoF

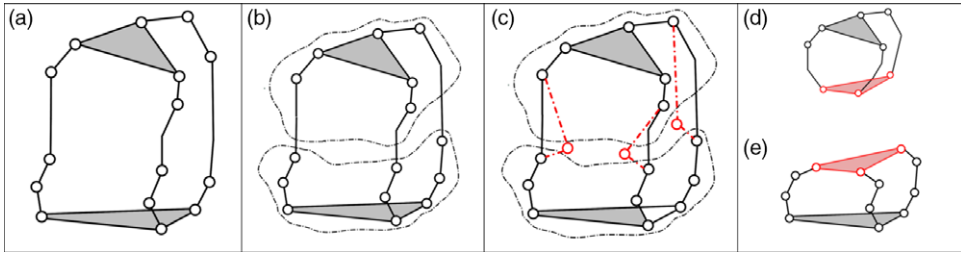


**Figure 2.** (a) Overconstrained manipulator with  $N$  DoF, (b) joints relation to two partial subspaces, (c) imaginary joints added to the manipulator, (d) second section parallel manipulator with  $J$  DoF, (e) first section parallel manipulator with  $N$  DoF.

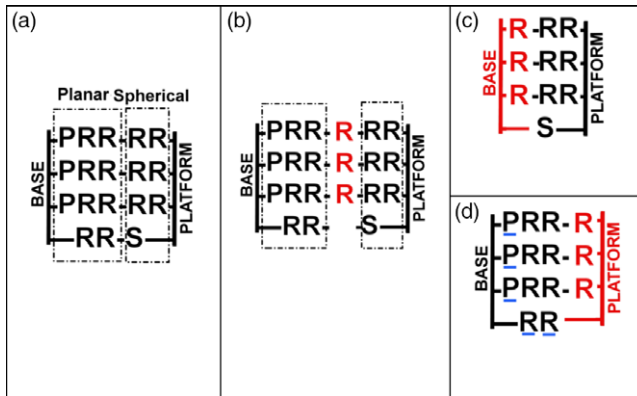


**Figure 3.** Decomposition method applied to 5 DoF parallel manipulator (a) OPM with subspace regions, (b) OPM with redundant imaginary joints, (c) 3 DoF passive spherical manipulator and (d) 5 DoF active planar manipulator.

(Fig. 2(d)) and a virtual base. This  $J$  DoF generates a motion about the geometry of the second section. The input of the manipulator in the second section comes from a part of the output of the first section manipulator. To formulate the number of motions that describe the platform motion, Eq. (1) is suggested. Where the number of motions belongs to the first subspace ( $M$ ) is found with the difference between the DoF of whole manipulator and second section manipulator.

$$M = N - J \tag{1}$$

### 3. Overconstrained Manipulator Analysis with Decomposition Method

Two OPMs with partial subspaces are newly created and analyzed to demonstrate the methodology’s aspects. The first one is a 5 DoF manipulator in subspace  $\lambda = 5$  and the second example is a 3 DoF manipulator in  $\lambda = 3$  subspace.

#### 3.1. 5 DoF PM in subspace $\lambda = 5$

The manipulator is designed with four legs, where three legs have  $\underline{PRR}(RR)$  joint combination and one leg has  $\underline{RRS}$  combination, as shown in Figs. 3(a) and 4(a). The joints in the planar region shown in Fig. 3(a) will be used to create the active planar manipulator. The joints shown in the spherical region will be used to create the passive spherical manipulator. For the manipulator,  $J$  is found as three because adding joints to three legs with  $\underline{PRR}(RR)$  do not create redundancy, and adding a joint to  $\underline{RRS}$  leg will

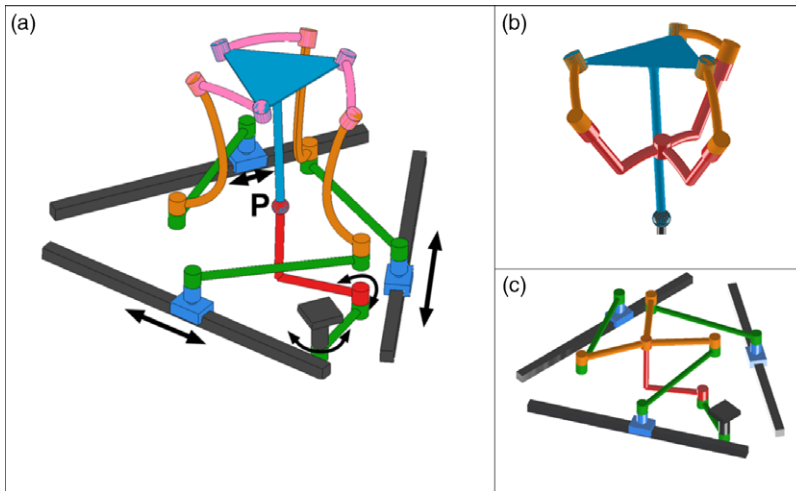


**Figure 4.** *Plano spherical  $\lambda = 5$  manipulator (a) actuators configuration, (b) passive spherical manipulator and (c) active planar manipulator.*

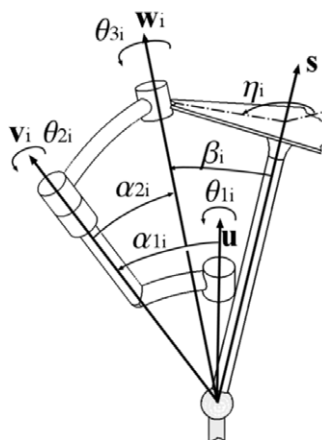


**Figure 5.** *Kinematic scheme of the imaginary spherical manipulator.*

create redundancy if connected with the spherical joint. In Fig. 3(b), three revolute joints are shown as imaginary joints. Revolute joints are selected due to the intersection motion between the planar and spherical subspaces is rotation, and the direction of the joints should be perpendicular to the planar subspace because the intersecting motion of two partial subspaces is in that direction. Figure 3(c) 3 DoF passive spherical manipulator and Fig. 3(d) 5 DoF active planar PM configuration are shown. The actuated joints in the system are shown as underlined in Fig. 3(d). The imaginary actuators of the spherical manipulator are imaginary joints. Platform translates along the plane in two directions and rotates around three directions. According to the Eq. (1), motion of the end effector that belongs to the lower platform (M) is found as two, which is the two translations of the lower platform.

*Inverse Kinematic Analysis  
Imaginary Primary Manipulator (Spherical Subspace)*

The upper part is a 3RRR spherical manipulator shown in Fig. 4(b), where three input revolute joints are inline. The kinematic scheme for the identical leg of the imaginary manipulator is shown in Fig. 5.

End-effector orientation of the manipulator is defined by  $\rho$ . It will be determined for a specific motion by using Euler angles in the  $R_{(z-y-z)}(\zeta, \xi, \psi)$  configuration, as  $\rho = Rot_z(\zeta) \cdot Rot_y(\xi) \cdot Rot_z(\psi)$ .

The vectors  $w_i = [w_{x,i} \ w_{y,i} \ w_{z,i}]^T$ , end effector joint positions for the upper manipulator will be found from Eqs. (2) and (3).

$$w_i = \rho \cdot Rot_z(\eta_i) \cdot Rot_y(\beta_i) \cdot s \tag{2}$$

The use of rotation matrices from a forward kinematics view describes the position of the vectors  $w_i$  in terms of the orientation of the input joint  $u = [0,0,1]^T$  and kinematic parameters of the upper manipulator as shown in Eq. (3).

$$w_i = Rot_z(\theta_{1i}) \cdot Rot_x(\alpha_1) \cdot Rot_z(\theta_{2i}) \cdot Rot_x(\alpha_2) \cdot u \tag{3}$$

The closure formed by Eqs. (2) and (3) gives three separate closure equations. The first two equations of Eq. (3) are used to find  $\theta_{1i}$  values for each leg of the mechanism.  $\theta_{1i}$  values will be used as output values for the secondary manipulator.

*Velocity analysis*

Let the angular velocity of the platform be  $\omega = [\omega_x \ \omega_y \ \omega_z]^T$  and the angular velocities of imaginary joints as  $\dot{\theta} = [\dot{\theta}_{11} \ \dot{\theta}_{12} \ \dot{\theta}_{13}]^T$ .

$\Omega$  is related to the orientation velocity matrix of the platform as

$$\Omega = \dot{s}s^{-1} = \begin{pmatrix} \mathbf{0} & -\omega_z & \omega_y \\ \omega_z & \mathbf{0} & -\omega_x \\ -\omega_y & \omega_x & \mathbf{0} \end{pmatrix} \tag{4}$$

Angular velocity of the rigid body is defined with the linear equations as,

$$\omega = u_i \dot{\theta}_{1i} + v_i \dot{\theta}_{2i} + w_i \dot{\theta}_{3i} \quad i = 1, 2, 3 \tag{5}$$

Where  $v_i = Rot_z(\theta_{1i}) \cdot Rot_x(\alpha_1) \cdot u$

Multiplying both sides of the Eq. (5) with  $(v_i \times w_i)$  will eliminate  $\dot{\theta}_{2i}$  and  $\dot{\theta}_{3i}$  from the constraint equation

$$\omega \cdot (v_i \times w_i) = u_i \cdot (v_i \times w_i) \dot{\theta}_i \quad i = 1, 2, 3 \tag{6}$$

Eq. (6) results in three linear equations that we can form a Jacobian matrix for the spherical manipulator.

$$J_{x,s} \omega = J_{q,s} \dot{\theta} \tag{7}$$

$$J_s \omega = \dot{\theta} \tag{8}$$

$$J_s = J_{q,s}^{-1} J_{x,s} \tag{9}$$

$$\text{Where } J_{q,s} = \begin{pmatrix} v_{1,x}w_{1,y} - v_{1,y}w_{1,x} & 0 & 0 \\ 0 & v_{2,x}w_{2,y} - v_{2,y}w_{2,x} & 0 \\ 0 & 0 & v_{3,x}w_{3,y} - v_{3,y}w_{3,x} \end{pmatrix},$$

$$J_{x,s} = \begin{pmatrix} v_{1,y}w_{1,z} - v_{1,z}w_{1,y} & -v_{1,x}w_{1,z} + v_{1,z}w_{1,x} & v_{1,x}w_{1,y} - v_{1,y}w_{1,x} \\ v_{2,y}w_{2,z} - v_{2,z}w_{2,y} & -v_{2,x}w_{2,z} + v_{2,z}w_{2,x} & v_{2,x}w_{2,y} - v_{2,y}w_{2,x} \\ v_{3,y}w_{3,z} - v_{3,z}w_{3,y} & -v_{3,x}w_{3,z} + v_{3,z}w_{3,x} & v_{3,x}w_{3,y} - v_{3,y}w_{3,x} \end{pmatrix}$$

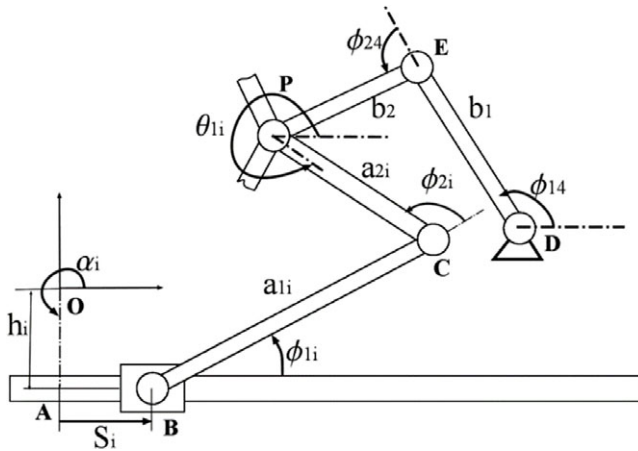


Figure 6. Kinematic scheme for the planar part of 5 DoF manipulator.

Imaginary secondary manipulator (planar subspace)

Planar manipulator

The imaginary secondary manipulator will be a planar 5 DoF redundant manipulator shown in Fig. 4(c). The manipulator’s output is the coordinates of point P and orientations of links joined at point P.

For the inverse kinematics of point P and joints at E and D loop closure equation will be,

$$\overline{OP} = \overline{OD} + \overline{DE} + \overline{EP} \tag{10}$$

It will result in two equations as

$$Px = Dx + b_1 \cos(\phi_{14}) + b_2 \cos(\phi_{14} + \phi_{24}) \tag{11}$$

$$Py = Dy + b_1 \sin(\phi_{14}) + b_2 \sin(\phi_{14} + \phi_{24}) \tag{12}$$

Solving these two equations will result in

$$\phi_{14} = \text{Atan2}(Dy - Py, Dx - Px) \pm \cos^{-1} \left( \frac{b_1^2 + b_2^2 + (Dx - Px)^2 + (Dy - Py)^2}{-2b_1 \sqrt{(Dx - Px)^2 + (Dy - Py)^2}} \right)$$

$$\phi_{24} = -\phi_{14} + \text{Atan2}(Py - Dy - b_1 \sin(\phi_{14}), Px - Dx - b_1 \cos(\phi_{14}))$$

the second loop closure equation (Eq. (13)) will be used to find actuator values for legs 1,2,3

$$\overline{OP} + \overline{PC} = \overline{OA} + \overline{AB} + \overline{BC} \tag{13}$$

$$Px + a_{2i} \cos(\theta_{1i}) = h_i \cos(\alpha_i) + S_i \cos\left(\alpha_i + \frac{\pi}{2}\right) + a_{1i} \cos\left(\alpha_i + \frac{\pi}{2} + \phi_{1i}\right) \tag{14}$$

$$Py + a_{2i} \sin(\theta_{1i}) = h_i \sin(\alpha_i) + S_i \sin\left(\alpha_i + \frac{\pi}{2}\right) + a_{1i} \sin\left(\alpha_i + \frac{\pi}{2} + \phi_{1i}\right) \tag{15}$$

Linear actuator values can be found as

$$S_i = -b \pm \sqrt{b^2 - 4c} \tag{16}$$

Where

$$b = (-2Py \cos(\alpha_i) + 2(Px \sin(\alpha_i) + a_{2i} \sin(\alpha_i - \theta_{1i})))$$

$$c = -a_{1i}^2 + a_{2i}^2 + h_i^2 + Px^2 + Py^2 - 2h_i Px \cos(\alpha_i) - 2a_{2i} h_i \cos(\alpha_i - \theta_{1i}) - 2h_i Py \sin(\alpha_i) + 2a_{2i} (Px \cos(\theta_{1i}) + Py \sin(\theta_{1i}))$$

*Velocity analysis*

For the planar manipulator, output velocities are stated with  $\dot{\mathbf{X}} = [\dot{\theta}_{11} \ \dot{\theta}_{12} \ \dot{\theta}_{13} \ \dot{P}_x \ \dot{P}_y]^T$  and the input velocities are shown with vector  $\dot{\mathbf{q}} = [\dot{S}_1 \ \dot{S}_2 \ \dot{S}_3 \ \dot{\phi}_{14} \ \dot{\phi}_{24}]^T$ .

$$Px + a_{2i}\cos(\theta_{1i}) = h_i\cos(\alpha_i) + S_i\cos\left(\alpha_i + \frac{\pi}{2}\right) + a_{1i}\cos\left(\alpha_i + \frac{\pi}{2} + \phi_{1i}\right) \tag{17}$$

$$Py + a_{2i}\sin(\theta_{1i}) = h_i\sin(\alpha_i) + S_i\sin\left(\alpha_i + \frac{\pi}{2}\right) + a_{1i}\sin\left(\alpha_i + \frac{\pi}{2} + \phi_{1i}\right) \tag{18}$$

From Eqs. (14) and (15),  $\phi_{1i}$  is eliminated to create a constraint equation

$$\begin{aligned} a_{1i}^2 = & h_i^2 + S_i^2 + Px^2 + Py^2 + a_{2i}^2 - 2Pxh_i\cos(\alpha_i) - 2h_i\cos(\alpha_i - \theta_{1i})a_{2i} - 2PxS_i\cos\left(\alpha_i + \frac{\pi}{2}\right) \\ & + 2Pxa_{2i}\cos(\theta_{1i}) - 2Pyh_i\sin(\alpha_i) - 2PyS_i\sin\left(\alpha_i + \frac{\pi}{2}\right) + 2Pya_{2i}\sin(\theta_{1i}) \end{aligned} \tag{19}$$

Moreover, it was derived by time for the velocity relations.

$$\begin{aligned} & [-Px - \cos(\theta_{1i})a_{2i} + \cos(\alpha_i)h_i - \sin(\alpha_i)S_i] \dot{P}_x + [-Py - \sin(\theta_{1i})a_{2i} + \sin(\alpha_i)h_i + \cos(\alpha_i)S_i] \dot{P}_y \\ & \times \dot{P}_y + a_{2i}[-Pycos(\theta_{1i}) + Pxsine(\theta_{1i}) + sine(\alpha_i - \theta_{1i})h_i + cosine(\alpha_i - \theta_{1i})S_i] \dot{\theta}_{1i} \\ & = [-Pycos(\alpha_i) + Pxsine(\alpha_i) + sine(\alpha_i - \theta_{1i})a_{2i} + S_i] \dot{S}_i \end{aligned} \tag{20}$$

Eqs. (10) and (11) is derived by time for further velocity relations

$$\dot{P}_x = (-b_1\sin(\phi_{14}) - b_2\sin(\phi_{14} + \phi_{24})) \dot{\phi}_{14} - b_2\sin(\phi_{14} + \phi_{24}) \dot{\phi}_{24} \tag{21}$$

$$\dot{P}_y = (b_1\cos(\phi_{14}) + b_2\cos(\phi_{14} + \phi_{24})) \dot{\phi}_{14} + b_2\cos(\phi_{14} + \phi_{24}) \dot{\phi}_{24} \tag{22}$$

$$J_{x,p}\dot{\mathbf{x}} = J_{q,p}\dot{\mathbf{q}} \tag{23}$$

$$J_p\dot{\mathbf{x}} = \dot{\mathbf{q}}$$

$$J_p = J_{q,p}^{-1}J_{x,p}$$

$$J_{q,p} = \begin{pmatrix} J_{q,p}^{1,1} & 0 & 0 & 0 & 0 \\ 0 & J_{q,p}^{2,2} & 0 & 0 & 0 \\ 0 & 0 & J_{q,p}^{3,3} & 0 & 0 \\ 0 & 0 & 0 & J_{q,p}^{4,4} & J_{q,p}^{4,5} \\ 0 & 0 & 0 & J_{q,p}^{5,4} & J_{q,p}^{5,5} \end{pmatrix}$$

Where,

$$J_{q,p}^{1,1} = -Pycos(\alpha_1) + Pxsine(\alpha_1) + sine(\alpha_1 - \theta_{11})a_{21} + S_1$$

$$J_{q,p}^{2,2} = -Pycos(\alpha_2) + Pxsine(\alpha_2) + sine(\alpha_2 - \theta_{12})a_{22} + S_2$$

$$J_{q,p}^{3,3} = -Pycos(\alpha_3) + Pxsine(\alpha_3) + sine(\alpha_3 - \theta_{13})a_{23} + S_3$$

$$J_{q,p}^{4,4} = (-b_1\sin(\phi_{14}) - b_2\sin(\phi_{14} + \phi_{24}))$$

$$J_{q,p}^{4,5} = -b_2\sin(\phi_{14} + \phi_{24})$$

$$J_{q,p}^{5,4} = (b_1\cos(\phi_{14}) + b_2\cos(\phi_{14} + \phi_{24}))$$

$$J_{q,p}^{5,5} = b_2\cos(\phi_{14} + \phi_{24})$$



$$J_{x,p} = \begin{pmatrix} J_{x,p}^{1,1} & 0 & 0 & J_{x,p}^{1,4} & J_{x,p}^{1,5} \\ 0 & J_{x,p}^{2,2} & 0 & J_{x,p}^{2,4} & J_{x,p}^{2,5} \\ 0 & 0 & J_{x,p}^{3,3} & J_{x,p}^{3,4} & J_{x,p}^{3,5} \\ 0 & 0 & 0 & 1 & 0 \\ 0 & 0 & 0 & 0 & 1 \end{pmatrix}$$

Where,

$$\begin{aligned} J_{x,p}^{1,1} &= a_{21} [-Pycos(\theta_{11}) + Pxs sin(\theta_{11}) + sin(\alpha_1 - \theta_{11}) h_1 + cos(\alpha_1 - \theta_{11}) S_1] \\ J_{x,p}^{2,2} &= a_{22} [-Pycos(\theta_{12}) + Pxs sin(\theta_{12}) + sin(\alpha_2 - \theta_{12}) h_2 + cos(\alpha_2 - \theta_{12}) S_2] \\ J_{x,p}^{3,3} &= a_{23} [-Pycos(\theta_{13}) + Pxs sin(\theta_{13}) + sin(\alpha_3 - \theta_{13}) h_3 + cos(\alpha_3 - \theta_{13}) S_3] \\ J_{x,p}^{1,4} &= -Px - cos(\theta_{11}) a_{21} + cos(\alpha_1) h_1 - sin(\alpha_1) S_1 \\ J_{x,p}^{1,5} &= -Py - sin(\theta_{11}) a_{21} + sin(\alpha_1) h_1 + Cos(\alpha_1) S_1 \\ J_{x,p}^{2,4} &= -Px - cos(\theta_{12}) a_{22} + cos(\alpha_2) h_2 - sin(\alpha_2) S_2 \\ J_{x,p}^{2,5} &= -Py - sin(\theta_{12}) a_{22} + sin(\alpha_2) h_2 + Cos(\alpha_2) S_2 \\ J_{x,p}^{3,4} &= -Px - cos(\theta_{13}) a_{23} + cos(\alpha_3) h_3 - sin(\alpha_3) S_3 \\ J_{x,p}^{3,5} &= -Py - sin(\theta_{13}) a_{23} + sin(\alpha_3) h_3 + cos(\alpha_3) S_3 \end{aligned}$$

Using Eqs. (7) and (22) recurrently, the velocity analysis of the whole manipulator can be done.

*Results of kinematic calculations*

The parameters for the 1st manipulator is selected with trial and error as follows,

$$\begin{aligned} \eta_1 = 0^\circ, \eta_2 = 120^\circ, \eta_3 = 240^\circ, \beta_i = 60^\circ; i = 1, 2, 3 \\ \alpha_1 = \alpha_2 = 75^\circ, Dx = 0, Dy = 75, b1 = 100, b2 = 100 \end{aligned}$$

To test the inverse kinematic solution for the manipulator and an objective motion is defined that has sinusoidal characteristic with different phase angles and frequencies. The objective motion of the orientation and translation of the end effector is shown in Fig. 7(a) and (b), respectively.

Using Eq. (3), the imaginary joint values are found for the objective orientation data and presented in Fig. 8.

These imaginary joint values are used as an objective function for the bottom manipulator. The actuated joints of the manipulator’s position and orientation are shown in Fig. 9(a) and (b), respectively.

The velocity relations for imaginary joints are tested by describing angular velocity at the end effector. The related imaginary joint velocities are found in Fig. 10(a), which will be used along with the sinusoidal translational velocity defined for the end effector to calculate the actuator velocities. The translational and angular velocities are found as presented in Fig. 10(b).

The decomposition method is also used to determine or design the workspace of the overconstrained manipulator. The determined workspace for the upper part of the 5 DoF manipulator is shown in Fig. 11(a), where the orientation is dexterous around  $\zeta$ . The range of the imaginary joints is calculated for  $\pm 20^\circ$  in all directions as,  $\theta_{11}$ :  $-0.55$  to  $+0.55$  radians,  $\theta_{12}$  from  $1.4$  to  $3.2$  radians,  $\theta_{13}$  from  $3.5$  to  $4.9$  radians. The workspace for the whole manipulator is then calculated using these ranges and presented in Fig. 11(b) and (c). It is seen that the  $\theta_{13}$  direction is dexterous.

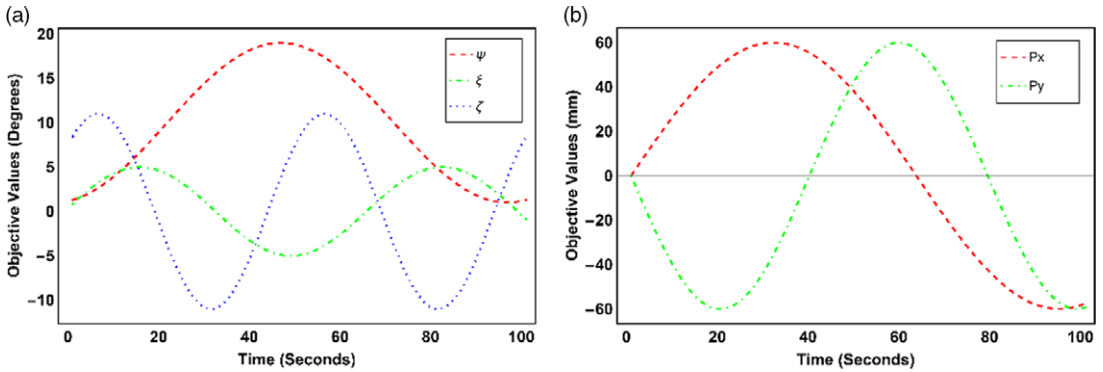


Figure 7. Objective values for 5 DoF manipulator (a) orientation and (b) translation.

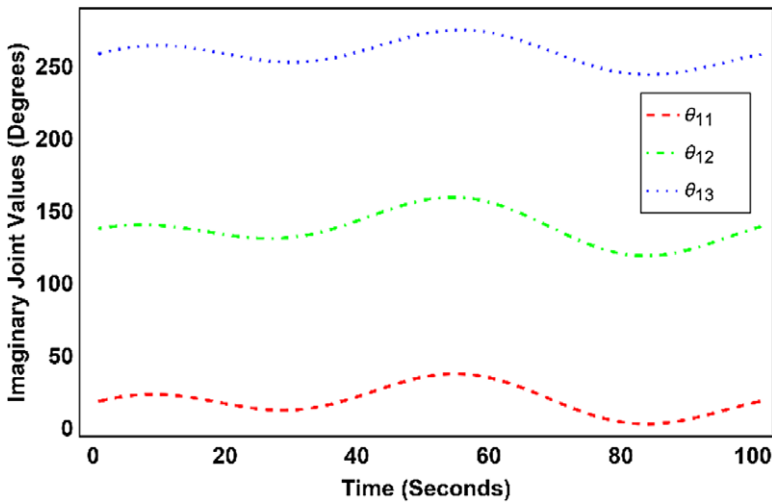


Figure 8. Calculated orientation values of imaginary joints.

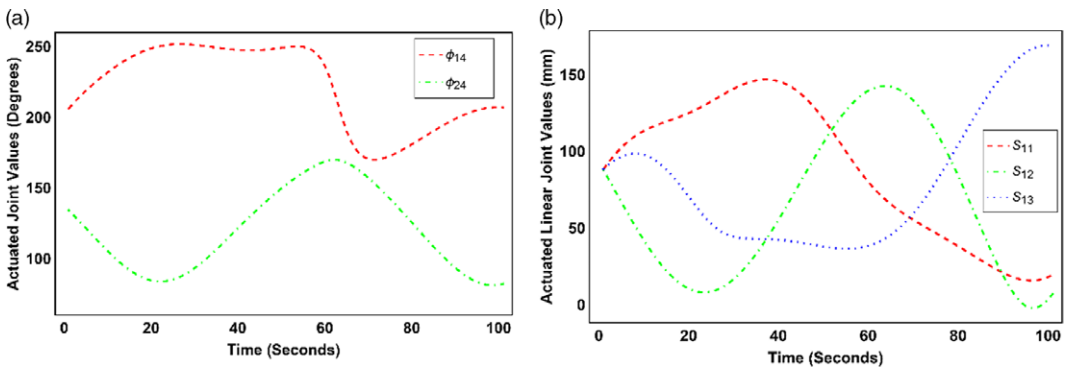
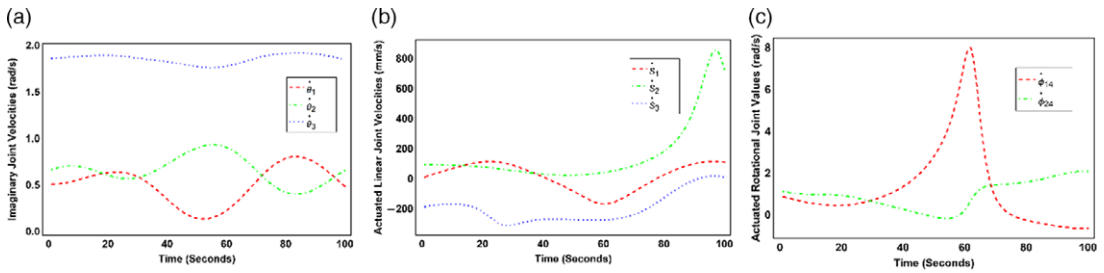
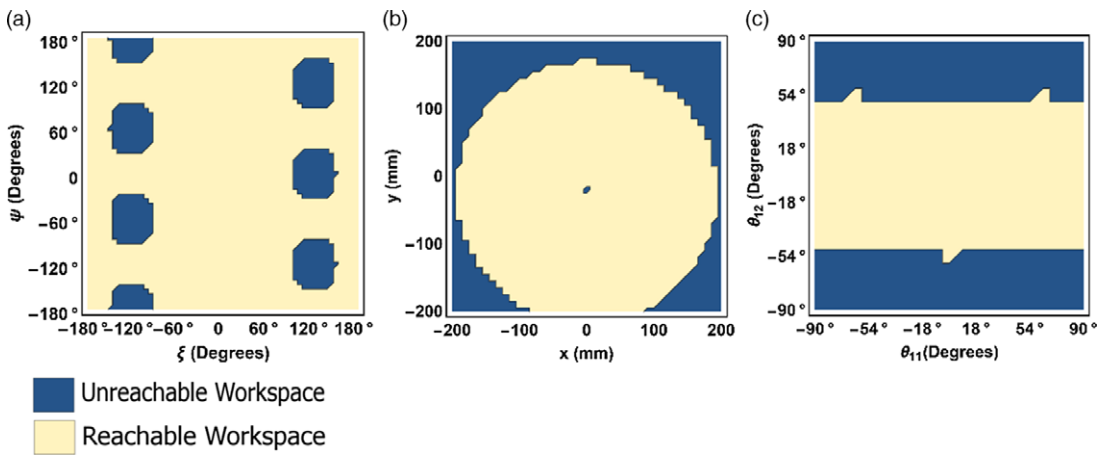


Figure 9. Calculated position and orientation values of actuated joints: (a) prismatic and (b) revolute.

For a design case of the manipulator for a better workspace, number of parameters in design should be 25. The use of imaginary joints helps divide the system into two parts and split the number of design parameters by 9 and 16. Thus, the design space is decreased from the order of 25 to 16 and 9. Also,



**Figure 10.** (a) Imaginary joints velocity, (b) linear actuator velocities and (c) angular actuator velocities.



**Figure 11.** (a) Individual workspace of the upper part of 5 DoF manipulator at  $\zeta = 0$ , (b) workspace of the manipulator for  $xy$  motion and (c) workspace for the imaginary joints.

the workspace of the imaginary joints shown in Fig. 11(c) can be used to set constraint equations for an optimization problem.

### 3.2. 3 DoF manipulator in subspace $\lambda = 3$

An overconstrained manipulator with 3 DoF is shown in Figs. 12(a) and 13(a). Manipulator has three legs, where two legs have PPR joint combination and one leg has PPH combination as shown in Fig. 12. The translational region's joints belong to the translational subspace, and joints in the cylindrical region belong to the cylindrical subspace. For the proposed manipulator, J is found as one because only one joint added to the PPH leg will not create redundancy for the upper passive manipulator. It is selected to be a prismatic joint due to the intersection motion of the planar with translation only space and cylindrical subspace is translational motion, and the direction of the prismatic joint should be coaxial with the intersection of these subspaces. Figure 12(c) 1 DoF cylindrical mechanism is seen, and Fig. 12(d) 3 DoF translational PM is seen. The actuated joints in the system are shown as underlined in Fig. 12(d). Using Eq. (1), motion of the end effector that belongs to the lower platform (M) is found as two related to the lower platform's translations.

The imaginary actuator of the cylindrical manipulator is an imaginary joint. Platform translates along the plane in two directions and rotates around one of the directions.

Three parameters define the manipulator's output—two translations along x and y axes as  $P_x$  and  $P_y$  and rotation around the y-axis as  $\phi$ . The upper part of the system is a one DoF mechanism with PHR

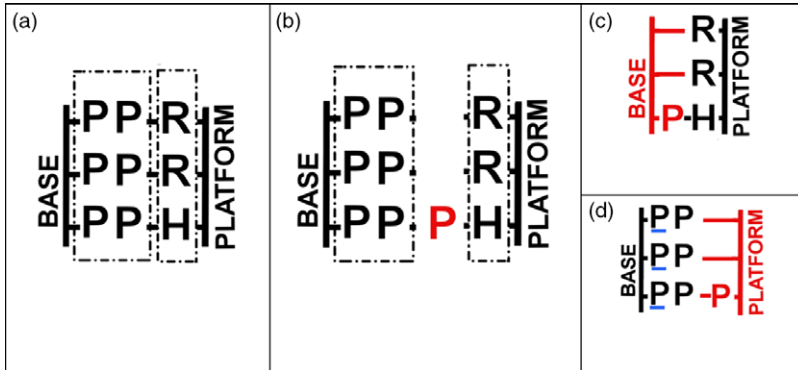


**Figure 12.** Decomposition method applied to 3 DoF parallel manipulator (a) 3 DoF overconstrained manipulator, (b) 3 DoF overconstrained manipulator with redundant imaginary joints, (c) 1 DoF passive cylindrical manipulator and (d) 3 DoF active translational manipulator.

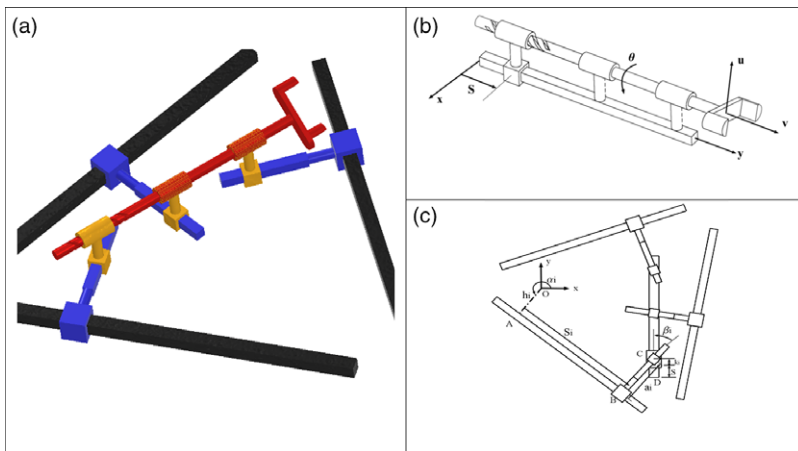


**Figure 13.** 3 DoF overconstrained manipulator (a) actuators configuration, (b) kinematics of the 1 DoF cylindrical mechanism and (c) kinematics of the 3 DoF planar manipulator.

joint configuration in cylindrical subspace. The output of the mechanism is  $\phi$ , and the input is  $S$  as shown in Fig. 13(b). The closure equation of the mechanism can be given as follows

$$\phi = \theta = s/p \tag{24}$$

where  $p$  is the pitch value for the helical joint.

From Eq. (24), the imaginary input value  $S$  can be calculated and derived by time to get the velocity equation

$$\dot{S} = p * \dot{\phi} \tag{25}$$

The secondary imaginary manipulator is a 3 DoF planar translational manipulator as shown in Fig. 13(c).

With the leg configuration as 2PP+PPP

$$OA + AB + BC + CP = OP \tag{26}$$

$$(h_i - a_i) \cos(\alpha_i) - S_i \sin(\alpha_i) - k_i \cos(\beta_i + \alpha_i) = P_x \tag{27}$$

$$(h_i - a_i) \sin(\alpha_i) - S_i \cos(\alpha_i) - k_i \sin(\beta_i + \alpha_i) = P_y \tag{28}$$

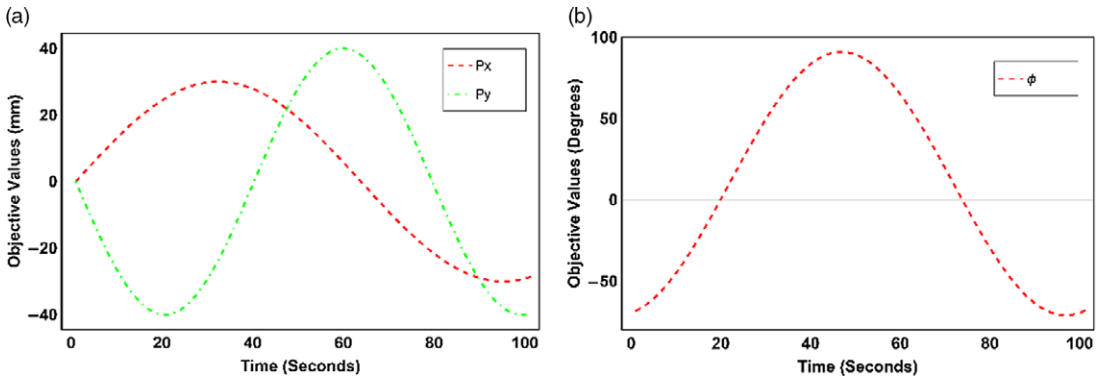


Figure 14. Displacement and orientation values of decided objective (a) translation and (b) orientation.

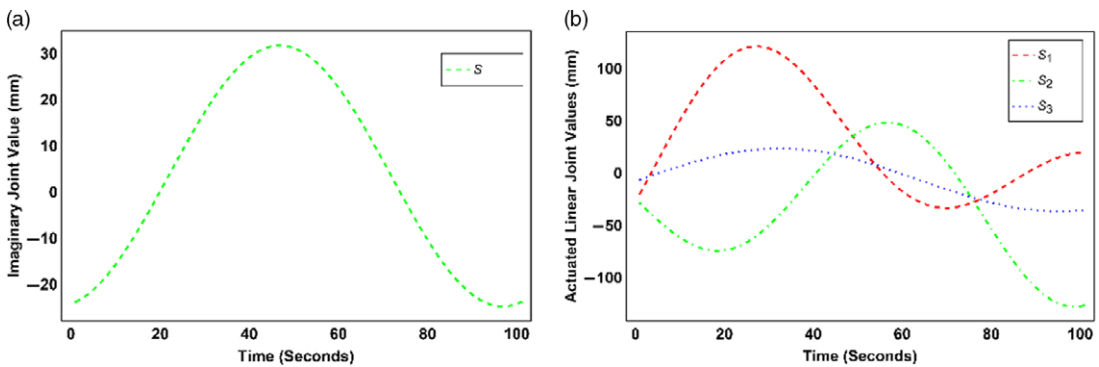


Figure 15. (a) Imaginary joint position changes of 3 DoF manipulator and (b) inverse kinematic position analysis of 3 DoF manipulator.

For link 1  $k_i = k_1 + S$

$$S_1 = [Py \cos(\alpha_1) - Px \sin(\alpha_1) + \sin(\beta_1)(k_1 + S)] / \cos(2\alpha_1)$$

$$S_2 = [Pycos(\alpha_2) - Pxsine(\alpha_2) + \sin(\beta_2)(k_2)] / \cos(2\alpha_2)$$

$$S_3 = [Pycos(\alpha_3) - Pxsine(\alpha_3) + \sin(\beta_3)(k_3)] / \cos(2\alpha_3)$$

Velocity analysis can be done by deriving the position equation by time. The velocity relation of the second example manipulator is found in Eq. (29).

$$\begin{bmatrix} \dot{S}_1 \\ \dot{S}_2 \\ \dot{S}_3 \end{bmatrix} = \begin{pmatrix} \frac{-\sin(\alpha_1)}{\cos(2\alpha_1)} & \frac{\cos(\alpha_1)}{\cos(2\alpha_1)} & \frac{\sin(\beta_1)}{\cos(2\alpha_1)} \\ \frac{-\sin(\alpha_2)}{\cos(2\alpha_2)} & \frac{\cos(\alpha_2)}{\cos(2\alpha_2)} & 0 \\ \frac{-\sin(\alpha_3)}{\cos(2\alpha_3)} & \frac{\cos(\alpha_3)}{\cos(2\alpha_3)} & 0 \end{pmatrix} \begin{bmatrix} \dot{P}_x \\ \dot{P}_y \\ \dot{S} \end{bmatrix} \quad (29)$$

The construction parameters for the second example manipulator is selected as,  $p = 20$  (constant pitch of the screw joint),  $\alpha_1 = 210^\circ$ ,  $\alpha_2 = 330^\circ$ ,  $\alpha_3 = 90^\circ$ ,  $\beta_1 = 45^\circ$ ,  $\beta_2 = 285^\circ$ ,  $\beta_3 = 165^\circ$ ,  $k_1 = 10$  mm,  $k_2 = 15$  mm,  $k_3 = 25$  mm with a  $\pm 400$  mm range of sliders.

Again a sinusoidal objective motion with different phase angles and frequencies was determined for the position and orientation of the 3 DoF manipulator, as shown in Fig. 14(a) and (b), respectively. The imaginary joint position  $S$  is found in Fig. 15(a), and the three slider values are calculated as shown in Fig. 15(b).

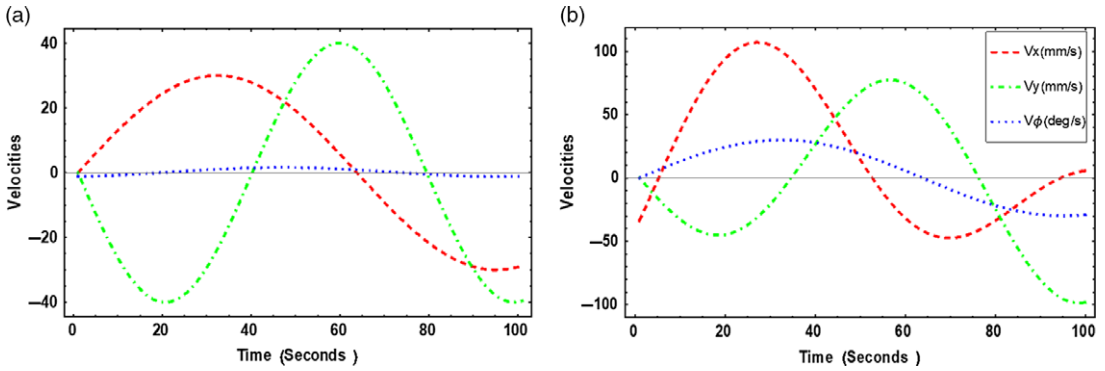


Figure 16. (a) Objective velocity of the platform and (b) calculated velocity of the actuator.

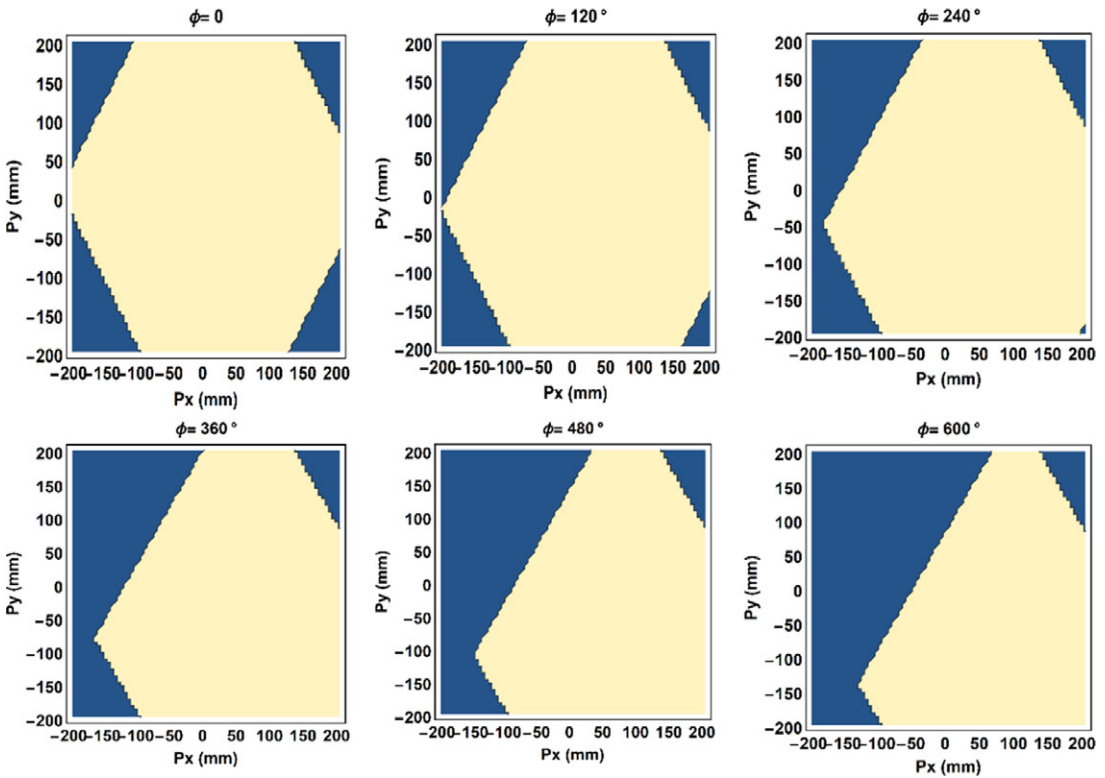


Figure 17. Workspace of the second example manipulator.

The velocity is determined and shown in Fig. 16(a), and corresponding velocity values are calculated as shown in Fig. 16(b).

The sliders' limits are selected as  $\pm 400$  mm, and the resulting workspace for  $\phi = 0, 120, 240, 360, 480, 600$  are presented in Fig. 17. It is seen that the workspace is shifting due to the rotation in the helical joint.

5. Discussion

The decomposition method is applied by dividing the system into lower subspace close loops rather than open loops. This unique approach shows several advantages in kinematic calculation simplicity,

understanding of the motion of the PM, workspace and singularity determination. With the help of decomposition, the manipulator is divided into two parts. Lower dimensional subsets can be investigated separately. Then singularities can be determined regarding the lower subspace and related motion. The use of the decomposition method is also helpful in means of calculations. Solving the kinematics for the manipulator commonly, they are needed to be dissected into arms and then for each arm, kinematic calculations should be done. Assuming the use of homogeneous transformation matrices for single arms of the system, some complex calculations should have been handled for spatial kinematics. For example, if this method is applied, the first example multiplication of five six by six homogeneous matrices should be solved. Also, dividing the motion into lower subspaces helps to identify the motion quickly. The use of the decomposition method shows that the workspace for the manipulator can be divided concerning the partial subspaces of the manipulator. Then individual parts can be calculated and investigated in means of workspace. The intersection of the workspace of the imaginary joints and the sub manipulator with the actuators will result in the actual workspace. The visualization of the separate workspace also helps in the interpretation in means of design. Among the two examples shown in the text, additional four manipulators are described in the appendix without detailed kinematics but just the use of the decomposition method.

## 6. Conclusion

The Decomposition method is defined and applied for two example manipulators. Results show that using the method and adding imaginary joints to the inverse position and velocity analysis with Jacobian can be achieved. Furthermore, it is also shown that the decomposition method will be a convenient tool for the design process of these types of manipulators for desired workspaces. Unlike most OPMs, the OPMs-PS have a clear definition for the subspace itself. Applicability of the method will open a way of research in this area of OPMs.

**Conflicts of Interest.** The author declares none.

**Financial Support.** This research received no specific grant from any funding agency, commercial or not-for-profit sectors.

**Supplementary Material.** To view supplementary material for this article, please visit <https://doi.org/10.1017/S0263574721001351>.

## References

- [1] J. P. Merlet, *Parallel Robots* (Springer Science & Business Media, 2005).
- [2] Z. Huang, Q. C. Li and H. F. Ding, *Theory of Parallel Mechanisms* (Springer, Dordrecht, 2012).
- [3] J. Angeles, *Fundamentals of Robotic Mechanical Systems* (Springer, 2014).
- [4] Z. Huang and Q. C. Li, "General methodology for type synthesis of symmetrical lower-mobility parallel manipulators and several novel manipulators," *Int. J. Rob. Res.* **21**(2), 131–145 (2002).
- [5] F. Gao, W. Li, X. Zhao, Z. Jin and H. Zhao, "New kinematic structures for 2-, 3-, 4-, and 5-DOF parallel manipulator designs," *Mech. Mach. Theory* **37**(11), 1395–1411 (2002).
- [6] G. Gogu, "Fully-Isotropic Over-Constrained Planar Parallel Manipulators," *In: 2004 IEEE/RSJ Int. Conf. Intell. Robot. Syst.*, vol. **4** (2004) pp. 3519–3524.
- [7] X. Kong and C. M. Gosselin, "Type synthesis of 5-DOF parallel manipulators based on screw theory," *J. Robot. Syst.* **22**(10), 535–547 (2005).
- [8] J. S. Dai, Z. Huang and H. Lipkin, "Mobility of overconstrained parallel mechanisms," *J. Mech. Des. Trans. ASME* **128**(1), 220–229 (2006).
- [9] C. C. Lee and J. M. Hervé, "Uncoupled actuation of overconstrained 3T-1R hybrid parallel manipulators," *Robotica* **27**(1), 103–117 (2009).
- [10] B. Hu, "Kinematically identical manipulators for the Exechon parallel manipulator and their comparison study," *Mech. Mach. Theory* **103**, 117–137 (2016).
- [11] O. Selvi, *Structural and Kinematic Synthesis of Overconstrained Mechanisms* (Izmir Institute of Technology, 2012).
- [12] Q. Yan, B. Li, Y. Li and X. Zhao, "Kinematics comparative study of two overconstrained parallel manipulators," *Math. Probl. Eng.* **2016** (2016).

- [13] B. Li, Y. Li and X. Zhao, “Kinematics analysis of a novel over-constrained three degree-of-freedom spatial parallel manipulator,” *Mech. Mach. Theory* **104**, 222–233 (2016).
- [14] L. Xu, G. Chen, W. Ye and Q. Li, “Design, analysis and optimization of Hex4, a new 2R1T overconstrained parallel manipulator with actuation redundancy,” *Robotica* **37**(2), 358–377 (2019).
- [15] A. Arian, M. Isaksson and C. Gosselin, “Kinematic and dynamic analysis of a novel parallel kinematic Schönflies motion generator,” *Mech. Mach. Theory* **147** (2020).
- [16] Q. Yan, B. Li, X. Zhao and Y. Li, “Comparative Stiffness Analysis of Two Over-Constrained Manipulators,” **In: ICARM 2016-2016 Int. Conf. Adv. Robot. Mechatronics** (2016) pp. 225–230.
- [17] O. Selvi and H. Al-Dulaimi, “Kinematic Analysis of a 5 dof Overconstrained Manipulator for Rehabilitation of Upper Extremite,” **In: IEEE Int. Conf. Acoust. Speech, Signal Process.** 2017, vol. **11**(2) (2015) pp. 52–69.
- [18] M. Sharifzadeh, A. Arian, A. Salimi, M. Tale Masouleh and A. Kalhor, “An experimental study on the direct & indirect dynamic identification of an over-constrained 3-DOF decoupled parallel mechanism,” *Mech. Mach. Theory* **116**, 178–202 (2017).
- [19] Z. Chen, L. Xu, W. Zhang and Q. Li, “Closed-form dynamic modeling and performance analysis of an over-constrained 2PUR-PSR parallel manipulator with parasitic motions,” *Nonlinear Dyn.* **96**(1), 517–534 (2019).
- [20] Y. Xu, W. Liu, J. Yao and Y. Zhao, “A method for force analysis of the overconstrained lower mobility parallel mechanism,” *Mech. Mach. Theory* **88**, 31–48 (2015).
- [21] W. L. Liu, Y. D. Xu, J. T. Yao and Y. S. Zhao, “Methods for force analysis of overconstrained parallel mechanisms: A review,” *Chinese J. Mech. Eng. (English Ed.)* **30**(6), 1460–1472 (2017).
- [22] O. Selvi and K. Yilmaz, “Inverse kinematics and dynamics of an overconstrained manipulator for upper extremity rehabilitation,” *Mech. Mach. Sci.* **46**, 437–443 (2017).
- [23] H. Liu, T. Huang, A. Kecskeméthy, D. G. Chetwynd and Q. Li, “Force/motion transmissibility analyses of redundantly actuated and overconstrained parallel manipulators,” *Mech. Mach. Theory* **109**(November 2016), 126–138 (2017).
- [24] Y. Xu, L. Lu, W. Liu, J. Guo, J. Yao and Y. Zhao, “Principle of force analysis of overconstrained parallel mechanisms considering link weight,” *Robotica* **37**(9), 1533–1544 (2019).
- [25] B. Hu and Z. Huang, “Kinetostatic model of overconstrained lower mobility parallel manipulators,” *Nonlinear Dyn.* **86**(1), 309–322 (2016).
- [26] C. Yang, Q. Li, Q. Chen and L. Xu, “Elastostatic stiffness modeling of overconstrained parallel manipulators,” *Mech. Mach. Theory* **122**, 58–74 (2018).
- [27] H. Zhang and H. Fang, “Stiffness characteristics analysis of a novel 3-DOF parallel kinematic machine tool,” *Int. J. Eng. Technol.* **10**(4), 346–354 (2018).
- [28] Q. Li, L. Xu, Q. Chen and X. Chai, “Analytical elastostatic stiffness modeling of overconstrained parallel manipulators using geometric algebra and strain energy,” *J. Mech. Robot.* **11**(3) (2019).
- [29] F. Zhao, Q. Yan, B. Li and J. Xie, “Workspace analysis of an over-constrained 2-RPU&SPR parallel manipulator,” *Math. Model. Eng. Probl.* **3**(2), 87–90 (2016).
- [30] H. Li and A. Nanc M, “A kinematics-based probabilistic roadmap method for closed chain systems,” *Algorithmic Comput. Robot.*, 243–251 (2020).
- [31] J. Cortés, T. Siméon and J. P. Laumond, “A Random Loop Generator for Planning the Motions of Closed Kinematic Chains Using PRM Methods,” **In: Proc. - IEEE Int. Conf. Robot. Autom.**, vol. **2**, May, pp. 2141–2146 (2002).
- [32] G. T. Bennett, “LXXVII. The parallel motion of Sarrut and some allied mechanisms,” *London, Edinburgh, Dublin Philos. Mag. J. Sci.* **9**(54), 803–810 (1905).